Proceedings of the ASME 2025
Fluids Engineering Division Summer Meeting
FEDSM 2025
July 27–30, 2025, Philadelphia, PA, USA

FEDSM2025-158275

ROBUST SOLUTION VERIFICATION EXPERIMENTS ON NONUNIFORM MESHES

Justin Weinmeister*
Nuclear Energy and Fuel Cycle Division
Oak Ridge National Laboratory
Oak Ridge, TN 37830
weinmeistejr@ornl.gov

Devina P. Sanjaya
Department of Mechanical, Biomedical,
and Aerospace Engineering
University of Tennessee, Knoxville
Knoxville, TN 37996
dsanjaya@utk.edu

ABSTRACT

The activities of verification, validation, and uncertainty quantification (VVUQ) provide a comprehensive means to assess the credibility of computational models. Within VVUQ, solution verification assesses numerical errors and evaluates whether the simulation is sufficiently accurate for its intended applications. As computational modeling gains traction in the development of complex, high-consequence systems, the need for robust solution verification intensifies, particularly because experimental data for these systems are often limited. This work examines improvements in the robustness of Richardson extrapolation (RE), a method commonly used in solution verification to study the discretization error of computational models using a power law. Nonuniform mesh refinement is discussed alongside other pollutants that affect the robustness of the power law model. Maximum likelihood estimation (MLE) is proposed as a robust strategy to address the uncertainty generated by nonuniform mesh refinement. An exploratory computational fluid dynamics (CFD) study of a 2D planar Poiseuille flow is conducted to determine if nonuniform mesh noise can be modeled with this MLE approach for more robust RE. [1]

NOMENCLATURE

f	Solution system response quantity
f_∞	Extrapolated solution system response quantity
g_1	Skewness
g_2	Excess kurtosis
h	Characteristic mesh size
p	Order of convergence
$\hat{p}$	Observed order of convergence
r	Mesh refinement ratio
α	Power series coefficients
Δs	Mesh edge spacing intervals
δ	Unstructured mesh noise
ε_h	Discretization error
μ	Mean of data
σ	Standard deviation

1 INTRODUCTION

Modern engineered systems such as nuclear reactors [1] or aircraft [2] can be categorized as complex, high-consequence systems. Complex systems are those for which formal descriptions do not exist or cannot be solved [2]. High-consequence systems are those for which failure can cause great harm or death [3]. Given the stakes, the research, design, and development of complex, high-consequence systems are aided by computational modeling such as computational fluid dynamics

*Address all correspondence to this author

(CFD) [4–8]. Computational models inherently contain numerical errors and uncertainties and may not represent the physical (real) system accurately. Thus, computational modeling, including CFD, must be accompanied with additional studies to ensure that simulation results can be used to make informed decisions.

The activities of verification, validation, and uncertainty quantification (VVUQ) allow engineers to make informed decisions. This paper focuses on solution verification, which aims to quantify all errors associated with a particular solution to a model. Often, the dominant error in CFD is the discretization error that results from solving a continuous problem on a discrete mesh [9, 10]. A classical method used to estimate discretization errors is Richardson extrapolation (RE), which involves computing solutions on multiple uniformly refined meshes. Although expensive, RE provides global error estimates of all system response quantities (SRQs) in a simulation; the term *global* refers to the accumulated discretization errors over the entire computational domain. Informed decision-making involving complex, high-consequence systems requires these global error estimates of SRQs for accurate VVUQ.

Other discretization error estimators exist and offer relative pros and cons compared to RE-based methods. The adjoint-based error estimates [11–13] can estimate the global errors of SRQs from a single mesh, although every SRQ requires a separate adjoint computation. Thus, the cost quickly increases with an increasing number of SRQs. Error transport equations provide global error estimates for all SRQs on a single mesh, but they require precise estimates of truncation errors [14] or mesh-induced residuals [15], which are not trivial to compute. Ultimately, there is still a place for all discretization error estimators today, with RE often serving as a baseline for newer single-mesh methods. The use of multiple meshes in RE gives insights into mesh dependence, allowing for further assessment of the credibility of the simulation results. Therefore, continued improvements in RE are beneficial, even outside the context of complex, high-consequence systems.

This paper focuses on improving the robustness of RE, specifically the ability of RE-based solution verification methods to handle pollutants from nonuniform refinement of unstructured meshes. To uniformly refine unstructured meshes, an integer refinement ratio of 2 or greater is needed. This makes RE-based methods prohibitively expensive for the unstructured meshes used to solve complex CFD models. A fractional refinement ratio reduces the computational cost but induces noise or errors due to nonuniform mesh refinement. This paper proposes that RE can be made more robust to this noise by selecting the proper maximum likelihood estimator (MLE) for the underlying uncertainty in nonuniform mesh refinement.

The remainder of this paper is organized as follows. Section 2 describes the theoretical foundation of RE with a focus on the standard power law model and its underlying assumptions. Section 3 discusses the impacts of pollutants in the RE-based error estimates on the overall robustness of RE-based solution verification methods. Sections 4 and 5 describe current and proposed robust approaches to improve RE in the presence of pollutants, respectively. Section 6 examines the hypothesized model of pollutants induced by the discrete mesh. Section 7 shows the results from a CFD simulation of a 2D planar Poiseuille flow. Section 8 concludes this analysis and discusses future research directions.

2 FOUNDATION OF RICHARDSON EXTRAPOLATION-BASED SOLUTION VERIFICATION METHODS

Fundamentally, discretization error is caused by solving a continuous problem on a discrete mesh. Hence, discretization error (ε_h) is the difference between the discrete solution (f_h) and the "true" (exact) solution f_∞:

$$\varepsilon_h = f_h - f_\infty. \tag{1}$$

The subscript ∞ refers to the "true" (exact) solution solved on a continuous domain, which is often conceptually thought of as the solution on a mesh with infinitely small cells or elements. Note that Eqn. (1) results in positive ε_h when $f_h > f_\infty$ and negative when $f_h < f_\infty$. In practice, $\varepsilon_h \neq 0$ because the cell or element size is always finite. Power series expansion gives a mathematical expression of discretization error as

$$\varepsilon_h = \alpha_1 h + \alpha_2 h^2 + \alpha_3 h^3 + ..., \tag{2}$$

where h is the characteristic mesh size, and α_n are the power series coefficients. Equation (2) serves as the mathematical foundation of RE-based solution verification methods. When the solutions are obtained on sufficiently fine meshes and in the asymptotic region of convergence, the discretization error is of the form $\varepsilon_h = \alpha h^p$, where α is constant for various h, and p is the theoretical order of convergence of the numerical scheme. RE-based solution verification was popularized in CFD by Roache through the Grid Convergence Index (GCI) method [16].

2.1 Solution Verification for CFD

For second-order CFD solvers, $p = 2$, and the first-order term in Eqn. (2) vanishes (i.e., $\alpha_1 = 0$):

$$f_h = f_\infty + \alpha_2 h^2 + O(h^3). \tag{3}$$

When f_h is in the asymptotic region of convergence, Eqn. (3) can be further simplified because $\alpha_2 = \alpha$ is constant for any h, and the higher order terms are negligible because $\alpha_2 h^2 \gg O(h^3)$. Hence,

$$f_h \approx f_\infty + \alpha h^2 \implies \varepsilon_h = \alpha h^2. \tag{4}$$

Because Eqn. (4) is quadratic, two solutions solved on two meshes from the same family (i.e., one finer and one coarser, with mesh refinement ratio r) are sufficient to solve for f_∞ and α. However, in practice, the *observed* order of convergence ($\hat{p}$) is not necessarily equal to the *theoretical* order of convergence (p). For example, factors such as shock waves, geometrical discontinuities, solution singularities, and linear approximations to curved boundaries degrade convergence [16]. So, in practice, Eqn. (5) is solved instead of Eqn. (4) when performing RE-based solution verification:

$$f_h = f_\infty + \alpha h^{\hat{p}} \implies \varepsilon_h = \alpha h^{\hat{p}} \tag{5}$$

Consequently, the following system of equations is formed to solve for f_∞, α, and $\hat{p}$:

$$\begin{cases} f_1 = f_\infty + \alpha h_1^{\hat{p}}, \\ f_2 = f_\infty + \alpha h_2^{\hat{p}}, \\ f_3 = f_\infty + \alpha h_3^{\hat{p}}, \end{cases} \tag{6}$$

where discrete solutions f_1, f_2, and f_3 are obtained using a CFD solver on a family of three uniformly refined meshes, h_1, h_2, and h_3. Uniform mesh refinement is a must to ensure discretization error from each element decreases by the same factor. However, the refinement ratio does not have to be an integer or constant (i.e., $r_{12} \neq r_{23}$). ASME V&V 20 [17] provides a more detailed explanation of solution verification, which includes the recommendation of generating more than three discrete solutions for complex problems. The overdetermined problem can be solved using the least-squares solution of Eqn. (5) per the work done by Eça and Hoekstra [18]. Section 4.2 discusses this least-square approach as one of robust error estimation methods. Ref. [19] interprets the ASME V&V 20 guidance as an iterative procedure and provides additional guidelines, which forms the basis for the solution verification software CFDverify [20] used to compute fits to the power law model in this work.

2.2 Example of Use

Figure 1 plots the power law model of the problem posed in Eqn. (6) for a synthetic second-order ($p = 2$) problem. The SRQ values are 9.97, 9.88, and 9.52 for mesh sizes of 0.1, 0.2, and 0.4, respectively. This data set results in $\hat{p} = 2$, $\alpha = -3$, and $f_\infty = 10.0$. Note that Fig. 1 depicts an ideal convergence behavior ($\hat{p} = p$), which is unlikely for practical CFD applications due to violations of the underlying assumptions of RE. Section 3 lists the pollutants in RE-based error estimates and explains the effect of the pollutants on the power law model described in Eqn. (5). This work also aims to investigate the underlying noise distributions due to these pollutants.

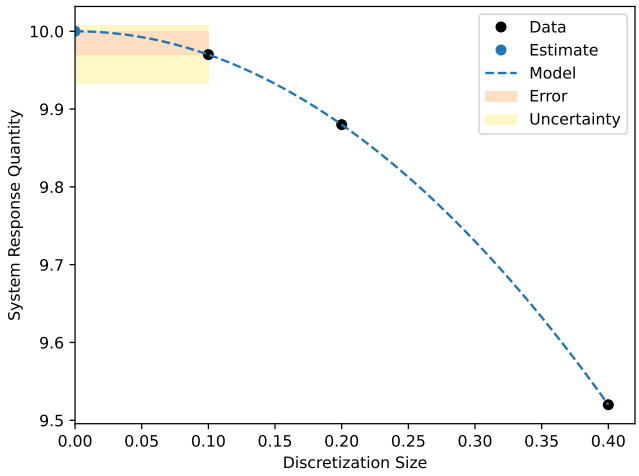

FIGURE 1. EXAMPLE OF RICHARDSON EXTRAPOLATION-BASED SOLUTION VERIFICATION.

3 POLLUTANTS IN RICHARDSON EXTRAPOLATION-BASED ERROR ESTIMATES

The underlying assumptions of RE are usually not fully satisfied in practical CFD settings. Although minor deviations from these assumptions may be acceptable, RE-based error estimates, like Eqn. (5), become less reliable with increasing deviations. Sources of pollutants in RE-based error estimates include:

1. The presence of discontinuities or irreducible first-order errors in the solution (e.g., $\alpha_1 \neq 0$),
2. Failure to obtain discrete solution in the asymptotic region of convergence (i.e., $\alpha h^2 \not\gg O(h^3)$ for second-order accurate schemes),
3. Pollution from iteration errors,
4. Nonuniform mesh refinement (i.e., r is not constant for all cells or elements), and
5. Switching between computational models (e.g., flux limiters and turbulence models) at different mesh refinement levels.

The following subsections discuss the implications of violating each of these assumptions.

3.1 Pollutants #1 & #2: Missing Terms in the Power Law Model

In the presence of discontinuities (e.g., shocks and sharp corners) the solution can not be expanded by a Taylor series, so Eqn. (5) is not a valid description of the discretization error. Likewise, irreducible first-order errors (e.g., straight approximations of curved surfaces) mean the first-order term in Eqn. (2) does not vanish. Hence, Eqn. (5) is missing an $\alpha_1 h$ term and is again an incomplete description of the discretization error. These additional errors can lead to nonmonotonic convergence behavior. For example, Roy employed a mixed-order model containing

both first- and second-order terms to account for the missing first-order terms in a problem with shocks and curved surfaces which caused oscillating convergence [21]. However, Roy also showed that in some cases, a first-order model alone could outperform the mixed-order model.

When constrained by computational costs, one level of the mesh refinement may be too coarse, causing the CFD simulation to fall short of the asymptotic regime. Like the issue with discontinuities discussed above, falling short of the asymptotic regime indicates that there are missing terms in Eqn. (5). For second-order accurate schemes, $\alpha h^2 \not\gg O(h^3)$, meaning the higher order terms in Eqn. (2) are now non-negligible. Consequently, the simplification of Eqn. (2) to (4) is no longer valid. Therefore, Eqn. (5) must include the higher order terms.

In either case, the missing terms in the power law model of the traditional RE (Eqn. (5)) indicate that there are missing convergence behaviors not captured in the single-term power series [17]. The current standard practice in the presence of pollutants #1 and #2 is to rely on the CFD analyst or practitioner to determine whether the fit based on the power law model is sufficient for reasonably estimating the discretization errors. Unfortunately, the CFD analyst or practitioner often finds it difficult to determine which solution data points are in the asymptotic regime, and more troubling, the discretization errors may be non-monotonic outside the simulated discretizations [22]. Hence, a "robust" regression in the presence of pollutants #1 and #2 would imply that the regression procedure includes model selection criteria [23] to determine if a simple model like Eqn. (5) outperforms a model with additional terms.

3.2 Pollutants #3 & #4: Fitting to Noise and Uncertainties

Discrete solutions (f_h) are inherently polluted by numerical errors such as round-off errors, iteration errors, and transported discretization errors. In a modern double-precision computation, round-off errors are usually nonsignificant, but iteration errors (pollutant #3) can be significant. The general practice is to reduce iteration errors to two or three orders of magnitude less than discretization errors [17, 24, 25]. In a calculation requiring only three significant digits of precision, the discretization errors should be of the order 10^{-4} of the SRQ. This means that the iteration errors should at least be of the order 10^{-6}; in the authors' experience, most CFD analysts or practitioners would require this level of iterative convergence to deem a solution "good enough." However, reducing iteration errors to the desired level can be difficult, and hence, iteration errors can pollute f_h.

Nonuniform mesh refinement (pollutant #4) is the primary concern of this work. As explained in Section 2.1, RE requires f_h from a family of *uniformly refined* meshes. Indeed, Eqn. (5) shows that each f_h is associated with a characteristic mesh size (h), which accounts for all cell or element sizes in the computational domain. For RE, the specific h value is not important, but the refinement ratio (r) between successive meshes in a family is important. Ideally, a constant r is applied to the entire domain so that all cells or elements experience the same discretization error reduction as the mesh is refined. For structured meshes, the prescribed point distributions are usually modified uniformly with an integer or noninteger r. For unstructured meshes, cells or elements are subdivided uniformly, although this often leads to large meshes, making the problem very expensive. Hence, in practice, CFD analysts or practitioners often apply uniform refinement to the mesh controls, knowing that the resulting meshes will not be precisely geometrically similar. This practice violates the underlying assumptions of RE. However, the mesh "families" are often "good enough" to conduct RE because the change in discretization error overshadows the noise from imprecise refinement. The limits of what constitutes a mesh family are not well studied. One study conducted by Carl Ollivier-Gooch on meshes generated for the Third American Institute for Aeronautics and Astronautics (AIAA) Drag Prediction Workshop (DPW III) defined a *refinement size quality* to compare the geometrical similarities of two meshes [26] and to assess the mesh pair appropriateness for mesh refinement study. This paper takes a different approach by investigating the impacts of noise from nonuniform mesh refinement on RE. Thus, "robust" regression in the presence of pollutants #3 and #4 would mean that the regression procedure considers the underlying statistics of imperfect refinement.

3.3 Pollutant #5: Changing the "True" (Exact) Solution

CFD solvers may switch between computational models at different mesh refinement levels. Consider the example of hybrid large-eddy simulation (LES)/Reynolds-averaged Navier–Stokes (RANS) as an example. The hybrid approaches use blending functions to switch from RANS in the near-wall regions to LES in the outer part of the boundary layer and locally separated flow regions [27]. These blending functions may depend on the mesh scale and the wall distance. Although this approach could reduce the cost of LES, switching between computational models can be problematic for RE. First, the "true" (exact) solution (f_∞) in Eqn (5) varies depending on the turbulence model used. Second, the dependence on the mesh scale and wall distance means that computational models may change at different mesh refinement levels, thus creating inconsistencies between meshes from the same family. All these factors violate the underlying assumptions of the traditional RE and can pose robustness issues. In the presence of pollutant #5, a "robust" regression would indicate that the regression procedure includes methods to bound f_∞.

3.4 Illustration of Impact on Overall Robustness

Figure 2 shows an example of deviations from the nominal model when normally distributed noise with a standard deviation

of 0.1% of f_∞ is present. In practice, the noise level and distribution are unknown, thus posing additional challenges in providing conservative discretization uncertainty estimates. Reducing noise in the error estimate requires either reducing the noise in the data or generating more data to quantify the noise. When uniform mesh refinement makes the problems computationally intractable, CFD analysts or practitioners must settle for other methods to create the best possible family of meshes and opt to generate more data. Regardless, more data points do not eliminate the noise from the nonuniform mesh refinements. Hence, there are benefits to understanding mesh noise and modifying traditional RE methods to account for the effects of mesh noise.

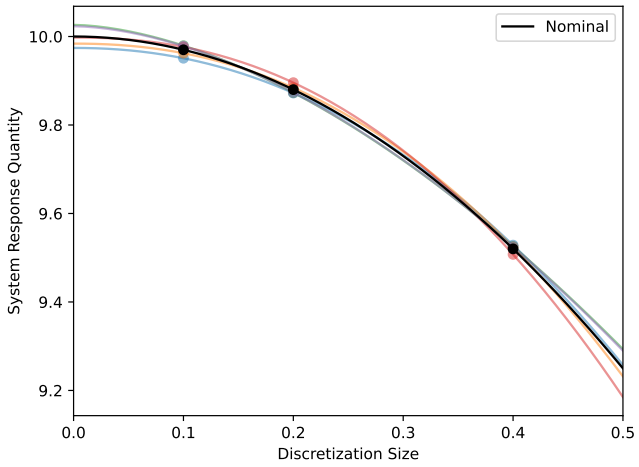

FIGURE 2. EXAMPLE OF RICHARDSON EXTRAPOLATION APPLIED TO NOISY DATA.

4 CURRENT ROBUST ESTIMATION METHODS

In the presence of pollutants, CFD analysts or practitioners need more than three solution data points to solve Eqn. (5) for the three unknowns: α, $\hat{p}$, and f_∞. Thus, instead of solving Eqn. (6) exactly, CFD analysts or practitioners are solving an overdetermined system through regression. Statistical treatment of data, including regression, requires an *estimator*, which is a procedure to obtain an *estimate* (i.e., a statistical solution) [28]. A "robust" estimator reduces sensitivity to minor deviations from the underlying assumptions [29]. This work seeks a robust estimator against noise resulting from nonuniform mesh refinements. The following subsections briefly review current methods to obtain robust RE-based error estimates.

4.1 Strategic Resampling (Jackknifing)

The simplest way to obtain robust RE-based error estimates based on four or more meshes is to resample the data into triplets (i.e., a subset of three) and solve them exactly; this approach is known as *jackknifing* [29]. To the best of the authors' knowledge, the first detailed study using this method is from 1997 by Celik and Karatekin [30], which qualitatively assesses the results of six triplets to ensure $\hat{p}$ and f_∞ are consistent. Ensuring $\hat{p}$ and p are consistent is also common when discussing the GCI method [17, 31]. Jackknifing can be performed systematically by evaluating the complete set of mesh triplets and drawing statistics from the final distribution. However, this method is sensitive to outliers; for example, three out of four jackknifed samples in a four-mesh study will be polluted by a single outlier.

4.2 Least-Squares Fitting

Eça and Hoekstra proposed a least-squares error (LSE) estimator to solve Eqn. (5). Compared to the jackknifing approach (Section 4.1), their LSE approach handles the coarsest mesh better [18], and it includes limits on $\hat{p}$, a factor of safety, and weights [32]. Their weighted LSE approach assigns weights of $w_i = \frac{1/h_i}{\sum_{i=1}^{N} 1/h_i}$, or the normalized reciprocal of the mesh size, to give greater weighting to finer meshes, thus providing a bias to reduce the errors of the finest mesh more than those of the coarse mesh. However, their study does not demonstrate that finer meshes have less noise when the family of meshes is nonuniformly refined. Furthermore, when SRQs on coarser meshes are more polluted than on finer meshes, the pollution may be from the missing terms in the standard power law model caused by not achieving the asymptotic regime (see Section 3.1 discussion of pollutant #2). In this case, development of model selection criteria is necessary, but only after the noise caused by nonuniform refinement is taken into account.

4.3 Ensemble of Regularization Strategies

Rider et al. proposed a method based on constrained optimization to improve the reliability of RE-based error estimates [33]. Their method focused on taking the "art" out of solution verification by employing an ensemble of regularization strategies to produce a robust estimate. For improved robustness, the method uses the median as the measure of central tendency and the median deviation as the uncertainty measure. This approach has a critical weakness in that it creates a fit by treating multiple norms equally. For example, if the underlying data have a Laplacian distribution, an estimate provided by an L_∞-norm estimator is likely to be poor because of the presence of outliers.

5 PROPOSED ROBUST ESTIMATION METHOD

This work proposes that robust RE-based error estimates for nonuniform mesh refinements should use MLE with the likelihood function chosen to match the expected distribution of SRQ values under nonuniform refinement. A thorough literature review revealed the lack of readily available methods to derive this distribution. As such, this work conducts an exploratory study of a SRQ distribution through experiment. The following subsec-

tions describe the statistical characteristics (i.e., mean, variance, skewness, and kurtosis) and noise distributions considered.

5.1 Characteristics of Distribution Functions

The *mean* of a distribution is its expected value, $\mu \equiv \mathrm{E}[\mathrm{SRQ}]$, or the arithmetic average of the data [34]. Of interest to this work is whether the mean of the data from nonuniformly refined meshes is the same as of uniformly refined meshes. If not, RE-based error estimates on nonuniform meshes contain a bias. If a bias is present, the median of the data should be used instead of the mean because the median measures the central tendency and minimizes the maximum bias in the estimate [29].

The *variance* of the data, $\sigma^2 = \mathrm{E}\left[(\mathrm{SRQ}-\mu)^2\right]$, measures the amount of noise from nonuniform mesh refinements that RE-based error estimates can handle before they become unreliable [34]; the variance is the square of the standard deviation. Based on prior work on iteration errors, a variance of two orders of magnitude or less than the discretization error is expected to have negligible effect [24], whereas the variance in the order of the discretization error will likely lead to unreliable results. This allowable variance applies to data obtained on the finest mesh and SRQs showing first-order convergence. For higher-order convergence, the allowable variance will scale with the mesh size.

Skewness is the third moment about the mean of a distribution, $(\mathrm{SRQ}-\mu)^3$, denoted by g_1, and it represents the asymmetry of the data. Data with positive skewness extend far above the mean, whereas data with negative skewness extend far below the mean [34]. Data with no skew are symmetric, like the normal distribution; for normally distributed data, the mean and the median will be the same. Hence, the magnitude of the skewness can determine when the median will be more robust than the mean.

Finally, the *kurtosis* — $(\mathrm{SRQ}-\mu)^4$, denoted as g_2 — of the data is informative to understand the best likelihood estimator to use for regression. In this work, excess kurtosis is used, or the raw kurtosis minus the kurtosis of a normal distribution [34]. Positive kurtosis implies that the distribution is leptokurtic and has fatter tails than the normal distribution; the Laplacian distribution is the canonical leptokurtic distribution. Negative kurtosis implies the distribution is platykurtic and has thinner tails; the uniform distribution is the canonical example.

5.2 Uniform Noise

A uniform distribution has finite support, zero skew, and is platykurtic. Uniformly distributed data has less extreme outliers than a normal distribution for the same variance and does not have a peak at the mean. The MLE for a uniform distribution minimizes the maximum error or the L_∞ norm of the data. A uniform distribution is described by Eqn. (7) with a as the lower bound and b as the upper bound.

$$f(x) = \begin{cases} \frac{1}{b-a}, & \text{for } a \le x \le b \\ 0, & \text{for } x < a \text{ or } x > b, \end{cases} \tag{7}$$

5.3 Normal Noise

A normal distribution is described by Eqn. (8),

$$f(x) = \frac{1}{\sqrt{2\pi\sigma^2}} e^{\frac{-(x-\mu)^2}{2\sigma^2}}, \tag{8}$$

where μ is the distribution mean, and σ is the standard deviation of the process f of variable x. A normal distribution is commonly observed in many real processes and is the canonical distribution function. Through visual inspection, the distribution of the refinement size quality between a pair of National Advisory Committee for Aeronautics (NACA) 0012 meshes in the work by Ollivier-Gooch [26] is normal. The MLE for a normal distribution minimizes the squared error or L_2 norm of the data.

5.4 Laplacian Noise

A Laplace distribution is described by Eqn. (9),

$$f(x) = \frac{1}{2b} e^{-\frac{|x-\mu|}{b}}, \tag{9}$$

where μ is the location parameter and equal to the mean, and b is the scale parameter and equal to $b = \sqrt{\sigma^2/2}$. The Laplace distribution can be thought of as two exponential distributions placed back to back along the mean. Like the normal distribution, the Laplace distribution is symmetric with zero skew; however, it is leptokurtic. The MLE for a Laplacian distribution minimizes the absolute error or L_1 norm of the data.

6 THEORETICAL MODELS OF MESH NOISE

The noise from nonuniform mesh refinement in the RE-based error estimates can be studied more effectively if the noise can be modeled mathematically. Two mesh noise models are hypothesized and tested on 2D planar Poiseuille flow. This process is neither analytic or exhaustive, but it should provide some evidence of the type of noise generated in these off-normal applications of RE-based solution verification methods.

Firstly, the noise can be modeled as constant across a given problem for all mesh resolutions. Equation (10),

$$f_h = f_\infty + \alpha h^{\hat{p}} + \delta, \tag{10}$$

describes this behavior, where δ is a random process. This random process would be described by a specific probability distribution. This distribution may theoretically be of any form and may be unique for every problem; if this is true, then developing generic robust regression methods is extremely difficult. However, if most CFD distributions can be well described by a common function, like those presented in Section 5, then developing a robust method is more tractable. Per this first hypothesized model, the variance in the SRQ values is expected to be the same for all mesh refinement levels.

The second hypothesized model is given in Eqn. (11),

$$f_h = f_\infty + \alpha h^{\hat{p}} + \alpha_\delta h^{\hat{p}_\delta}, \tag{11}$$

where α_δ is a random noise constant. In contrast to Eqn.(10), $\delta = \alpha_\delta h^{\hat{p}_\delta}$, or δ varies with mesh refinement levels. Equation (11) still approaches the impacts of mesh noise on RE as the addition of a random process; however, the random process is also a function of the mesh refinement itself. Note that the model assumes the functional relationship is the same as for the discretization error, though the mesh noise may have a unique order ($\hat{p}_\delta \neq \hat{p}$).

This analysis considers these two noise models to determine whether it is more likely that the noise generated from nonuniform mesh families is a function of refinement or not. It is reasonable that the functional relationship will not be exactly $h^{\hat{p}}$ if the noise is a function of the mesh size. However, literature does not reveal other orders or bases for the functional relationship.

7 RESULTS

This work uses a 2D planar Poiseuille flow to study the underlying mesh noise distributions. The channel is 1 m long and 0.1 m tall ($d_h = 0.2$ m). It is filled with a unit density fluid ($\rho = 1$ kg/m^3) with a kinematic viscosity of $\nu = 0.002$ m^2/s, a thermal conductivity of $k = 0.0001$ W/m-K, and a specific heat capacity of $c_p = 0.05$ J/kg-K. The resulting flow has a Reynolds number ($\mathrm{Re} = uL/\nu$) of 10 and a Prandtl number ($\mathrm{Pr} = c_p\mu/k$) of 1. The SRQ of interest is the temperature at the center of the channel. The thermal entrance length for a laminar flow is given by $l_t = 0.05\mathrm{RePr}$ and is 0.5 m for this flow; as such, the flow is fully developed at the SRQ point. Figure 3 shows a diagram of the geometry with dimensions, boundary conditions, and the point of interest at $[0.5, 0]$ m. The laminar inlet boundary condition specifies the velocity at the inlet using a fully developed laminar flow profile at a constant temperature of 300 K.

The flow was solved using VERTEX-CFD, an incompressible Navier-Stokes solver developed at Oak Ridge National Laboratory (ORNL) [35]. VERTEX-CFD uses a continuous-Galerkin method to discretize the governing equations and artificial compressibility to couple the pressure and velocity fields.

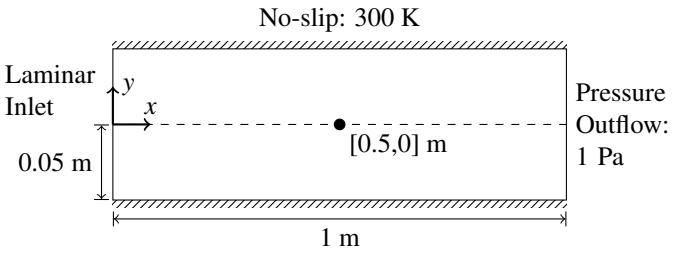

FIGURE 3. DIAGRAM OF PLANAR POISEUILLE FLOW.

The flow solutions were obtained using a set of linear basis functions to achieve second-order ($p = 2$) theoretical convergence. VERTEX-CFD is a transient solver, so solutions were obtained at a final time of $t = 100$ s with steady-state behavior establishing at approximately 20 s for an initial velocity field of $[0.1, 0]$ m/s. Iterative convergence was determined based on a mean L_2-norm over the mass and momentum equations of 1×10^{-10} at each time step. Time steps were chosen adaptively with an initial time step $\Delta t = 1 \times 10^{-2}$ s and a maximum Courant–Friedrichs–Lewy (CFL) limit of 100.

7.1 Uniform Mesh Refinement

Reference results were obtained on 40 uniformly refined square quadrilateral meshes. The mesh spacing was set by the number of divisions for the channel height (Δs) and ranges from 10 to 49 for the uniform refinement study. Each uniform mesh has a total of $\Delta s \times 10\Delta s$ elements. Figure 4 shows the excellent fit of the power law model to the data with $\hat{p} = 2.0196$ and $f_\infty = 300.1497$ K. The estimated error for the finest mesh ($\Delta s = 49$) is $\varepsilon_h = 2.1992 \times 10^{-4}$ K.

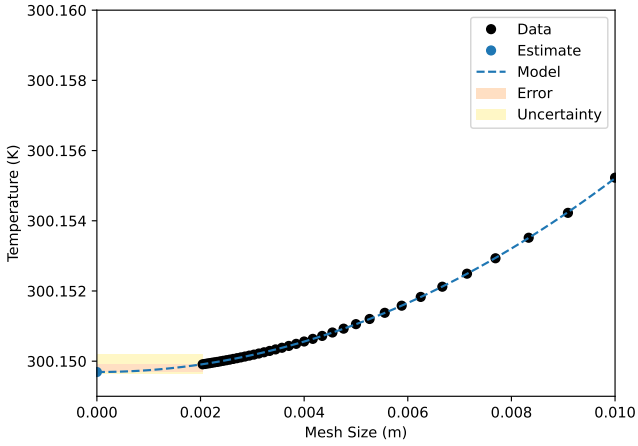

FIGURE 4. UNIFORM MESH REFINEMENT CONVERGENCE OF TEMPERATURE AT CENTER OF CHANNEL.

7.2 Nonuniform Mesh Refinement

Nonuniform meshes were generated with HUMOR (High-order Unstructured Mesh for Oak Ridge), a meshing tool developed at ORNL by Steve Karman. HUMOR distributes mesh points through a particle interaction model before tessellating them into a mesh [36]. Critical to this work, HUMOR can produce unique meshes of nearly identical quality. To create unique meshes of consistent quality, odd-numbered spacing intervals were chosen, the "jiggle" operation was applied during refinement, and the number of smoothing steps between mesh refinement operations was varied between 490 and 510. The frequency of refinement steps has a minor impact on the total element count, but it was essential to creating unique meshes.

A vertex was placed at $[0.5, 0]$ m to eliminate interpolation errors in the extracted SRQ values for each mesh. For meshing, the geometry was divided into upper and lower blocks with a line along $y = 0$ m divided at $x = 0.5$ m. This forced HUMOR to mesh the channel as two blocks with coincident vertices along the channel centerline. The mesh blocks were then combined before solving the flow solutions. As in the uniform mesh refinement test case, the mesh size was set relative to the channel height with edge spacings of $\Delta s = [9, 11, 13, 17, 27, 49]$. No volume growth rate was applied, so the mesh was generated with a uniform Riemannian metric field of size Δs. Elements in the generated meshes are close to isotropic triangles, whereas the elements in the uniform refinement study are exclusively square quadrilaterals. For each mesh size, 20 distinct nonuniform meshes were created and solved.

Figure 5 shows the individual data points for each of the nonuniform mesh solutions; the resulting RE parameters are $\hat{p} = 2.61$ and $f_\infty = 300.1498$ K with an estimated error of $\varepsilon_h = 1.11 \times 10^{-6}$ K at $\Delta s = 49$. Note, the observed order ($\hat{p} = 2.61$) is much higher than the theoretical order ($p = 2$) and exceeds the ad hoc limits used in many solution verification methods [32, 33] to prevent nonconservative error estimates. The estimated error for the finest mesh level ($\Delta s = 49$) is $\varepsilon_h = 1.5545 \times 10^{-4}$ K; this is 29% lower than the uniform refinement case and likely due to the higher observed order. Also, unlike the uniform refinement case, scatter is seen in the convergence data due to the nonuniform refinement of the domain. The most obvious result from Fig. 5 is that Eqn. (11) better describes the noise than Eqn. (10). This is supported by the summary statistics reported in Tab. 1, which shows that the standard deviation decreases with mesh refinement. The power law, Eqn. (5), was fit to the standard deviations in column 4 of Tab. 1 to estimate the final term in Eqn. (11); the resulting RE parameters are $\hat{p}_\delta = 4.14$ and $f_\infty = 9 \times 10^{-6}$ K. Compared, $\hat{p}_\delta$ is 59% higher than $\hat{p}$.

Looking closer at the data, the mean and median SRQ for each refinement level match closely, and the skewness does not have a definitive trend with three levels showing slight negative skewness and three slight positive skewness. Hence, the results indicate that the underlying distributions of the noise due to nonuniform mesh refinement are not asymmetric. Finally, the kurtosis data in Tab. 1 suggests that the data is platykurtic with all six refinement levels showing negative excess kurtosis. However, both of these observations are far from conclusive; further analysis is necessary.

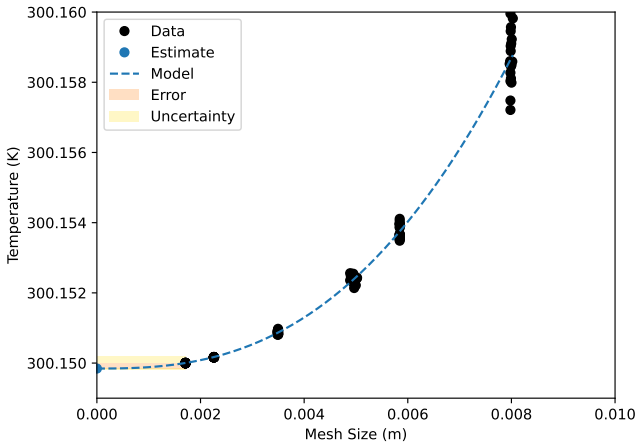

FIGURE 5. NONUNIFORM MESH REFINEMENT CONVERGENCE OF TEMPERATURE AT THE CENTER OF CHANNEL.

Next, bootstrapping is necessary for analyzing the effects of nonuniformly refined meshes in a typical solution verification study, where only one mesh per discretization level is used. Table 2 shows the statistics for 10,000 bootstrapped samples; a mesh was randomly selected from the six refinement levels and sampling with replacement was employed. First, the mean and median of $\hat{p}$ are close to the order achieved with the full data set, as shown in Tab. 1. However, the standard deviation of $\hat{p}$ is relatively high at 10% of the nominal value. The skewness of $\hat{p}$ is slightly negative and its excess kurtosis is negative. Taken together, the average bootstrapped $\hat{p}$ matches the full data set with a wide distribution but few outliers. In contrast, f_∞ and ε_h show significant variation, skew, and outliers. The standard deviation of ε_h is 61% of the mean value or the same order of magnitude. Also, f_∞ and ε_h have higher skewness than $\hat{p}$ and are leptokurtic. As such, the estimated errors of the CFD solutions have asymmetric distributions and tend to have outliers than normally distributed data despite $\hat{p}$ and the meshes not showing this behavior.

8 CONCLUSION

This work hypothesizes that RE-based discretization error estimators can be more robust for nonuniform mesh refinements (including unstructured meshes) by choosing a particular distribution for the mesh noise and employing MLE. To do so, sources of pollutants in the RE-based error estimates were classified, and their impacts on the power law model, as shown in Eqn. (5), analyzed. A literature review revealed the lack of foundation for

TABLE 1. STATISTICS OF TEMPERATURE (IN KELVIN) FOR 20 NONUNIFORMLY REFINED MESHES

Δs	μ	Median	σ	g_1	g_2
9	300.158 67	300.158 57	$7.289\,97 \times 10^{-4}$	−0.054 32	−0.502 48
11	300.153 76	300.153 66	$2.107\,83 \times 10^{-4}$	0.202 61	−1.533 16
13	300.152 38	300.152 38	$1.096\,18 \times 10^{-4}$	−0.275 29	−0.243 74
17	300.150 88	300.150 88	$4.695\,96 \times 10^{-5}$	0.118 88	−0.792 17
27	300.150 17	300.150 17	$4.904\,17 \times 10^{-6}$	−0.240 46	−0.662 11
49	300.150 00	300.150 00	$5.597\,10 \times 10^{-6}$	0.156 73	−0.723 44

TABLE 2. STATISTICS OF BOOTSTRAPPED DISCRETIZATION ERROR SAMPLES

Parameter	μ	Median	σ	g_1	g_2
$\hat{p}$	2.596 77	2.601 25	0.263 68	−0.121 17	−0.339 62
f_∞ [K]	300.149 83	300.149 84	$1.035\,99 \times 10^{-4}$	−0.647 12	0.370 75
ε_h [K]	$1.696\,64 \times 10^{-4}$	$1.561\,09 \times 10^{-4}$	$1.036\,52 \times 10^{-4}$	0.646 52	0.370 21

studying mesh noise in the context of RE-based solution verification for CFD, so two theoretical models of mesh noise were proposed and analyzed under the context of MLE. An exploratory study of nonuniform refinement for a 2D planar Poiseuille flow suggests that mesh noise is a random process which decreases with mesh refinement. Further, while the underlying noise due to nonuniform mesh refinement appears symmetric with few outliers, the estimated errors in CFD solutions show asymmetry and significant outliers. All in all, this work indicates that modeling mesh noise may improve the robustness of RE-based methods. However, further analysis is needed to determine the exact underlying distribution of mesh noise.

ACKNOWLEDGMENT

The authors would like to thank Marco Delchini for his help in setting up VERTEX-CFD models and Lawton Shoemake for his help with HUMOR.

REFERENCES

[1] Fullwood, R. R., and Hall, R. E., 1988. *Probabilistic Risk Assessment in the Nuclear Power Industry: Fundamentals & Applications*. Pergamon.

[2] Flumerfelt, S., Schwartz, K. G., Mavrism, D., and Briceno, S., 2019. *Complex Systems Engineering - Theory and Practice*. American Institute of Aeronautics and Astronautics (AIAA), Reston, VA, USA.

[3] Frank, M. V., 2008. *Choosing Safety - A Guide to Using Probabilistic Risk Assessment and Decision Analysis in Complex, High-Consequence Systems*. Resources for the Future, Washington DC, USA.

[4] Fang, J., Shaver, D. R., Tomboulides, A., Min, M., Fischer, P., Lan, Y.-H., Rahaman, R., Romano, P., Benhamadouche, S., Hassan, Y. A., et al., 2021. "Feasibility of Full-Core Pin Resolved CFD Simulations of Small Modular Reactor with Momentum Sources". *Nuclear Engineering and Design,* ***378***, p. 111143.

[5] Boyd, C., 2016. "Perspectives on CFD Analysis in Nuclear Reactor Regulation". *Nuclear Engineering and Design,* ***299***, pp. 12–17.

[6] Sanjaya, D., Fidkowski, K., and Tobasco, I., 2014. "Adjoint-Accelerated Statistical and Deterministic Inversion of Atmospheric Contaminant Transport". *Computers & Fluids,* ***100***, pp. 291–307.

[7] McDaniel, D. R., Cummings, R. M., Bergeron, K., Morton, S. A., and Dean, J., 2009. "Comparisons of Computational Fluid Dynamics Solutions of Static and Manoeuvring Fighter Aircraft with Flight Test Data". *Proceedings of the Institution of Mechanical Engineers, Part G: Journal of Aerospace Engineering,* ***223***(4), pp. 323–340.

[8] Johnson, F. T., Tinoco, E. N., and Yu, N. J., 2005. "Thirty Years of Development and Application of CFD at Boeing Commercial Airplanes, Seattle". *Computers & Fluids,* ***34***(10), pp. 1115–1151.

[9] Roy, C., 2010. "Review of Discretization Error Estimators in Scientific Computing". In 48th AIAA Aerospace Sciences Meeting Including the New Horizons Forum and

Aerospace Exposition, American Institute of Aeronautics and Astronautics.

[10] Mavriplis, D. J., 2005. "Grid Resolution Study of a Drag Prediction Workshop Configuration Using the NSU3D Unstructured Mesh Solver". In 23rd AIAA Applied Aerodynamics Conference, American Institute of Aeronautics and Astronautics.

[11] Venditti, D. A., and Darmofal, D. L., 2000. "Adjoint Error Estimation and Grid Adaptation for Functional Outputs: Application to Quasi-One-Dimensional Flow". *Journal for Computational Physics,* ***164***(1), pp. 204–227.

[12] Fidkowski, K. J., and Darmofal, D. L., 2011. "Review of Output-Based Error Estimation and Mesh Adaptation in Computational Fluid Dynamics". *AIAA Journal,* ***49***(4), pp. 673–694.

[13] Balan, A., Park, M. A., Wood, S. L., Anderson, W. K., Rangarajan, A., Sanjaya, D. P., and May, G., 2022. "A Review and Comparison of Error Estimators for Anisotropic Mesh Adaptation for Flow Simulations". *Computers & Fluids,* ***234***, p. 105259.

[14] Celik, I., and Hu, G., 2004. "Single Grid Error Estimation Using Error Transport Equation". *Journal of Fluids Engineering,* ***126***(5), pp. 778–790.

[15] Williams, B., and Shih, T., 2010. "Estimating Grid-Induced Errors in Unsteady CFD Solutions Using a Discrete Error Transport Equation". In 48th AIAA Aerospace Sciences Meeting Including the New Horizons Forum and Aerospace Exposition, p. 1361.

[16] Roache, P. J., 1994. "Perspective: A Method for Uniform Reporting of Grid Refinement Studies". *Journal of Fluids Engineering,* ***116***(3), pp. 405–413.

[17] AMERICAN SOCIETY FOR MECHANICAL ENGINEERS, 2009. *Standard for Verification and Validation in Computational Fluid Dynamics and Heat Transfer (ASME V&V 20-2009)*.

[18] Eça, L., and Hoekstra, M., 2002. "An Evaluation of Verification Procedures for CFD Applications". In 24th Symposium on Naval Hydrodynamics.

[19] Weinmeister, J., and Sanjaya, D. P., 2024. "Successive Procedure for Solution Verification Based on User Needs". In Proceedings of the ASME 2024 Verification, Validation, and Uncertainty Quantification Symposium, American Society of Mechanical Engineers, p. V001T07A001.

[20] Weinmeister, J., and Sanjaya, D. P., 2025. "An Open-Source Python Package for CFD Solution Verification". In Proceedings of the ASME 2025 Verification, Validation, and Uncertainty Quantification Symposium, American Society of Mechanical Engineers.

[21] Roy, C. J., 2003. "Grid Convergence Error Analysis for Mixed-Order Numerical Schemes". *AIAA Journal,* ***41***(4), pp. 595–604.

[22] Eça, L., Kerkvliet, M., and Toxopeus, S., 2023. "Attaining the Asymptotic Range in RANS Simulations". In ASME 2023 Verification, Validation, and Uncertainty Quantification Symposium, Vol. 86748, p. V001T02A002.

[23] Hastie, T., Tibshirani, R., and Friedman, J., 2009. *The Elements of Statistical Learning*, 2nd ed. Springer.

[24] Eça, L., and Hoekstra, M., 2009. "Evaluation of Numerical Error Estimation Based on Grid Refinement Studies with the Method of the Manufactured Solutions". *Computers & fluids,* ***38***(8), pp. 1580–1591.

[25] Oberkampf, W. L., and Roy, C. J., 2010. *Verification and Validation in Scientific Computing*. Cambridge University Press, Cambridge.

[26] Ollivier-Gooch, C., 2009. "Assessing Validity of Mesh Refinement Sequences with Application to DPW-III Meshes". In 47th AIAA Aerospace Sciences Meeting including The New Horizons Forum and Aerospace Exposition, American Institute of Aeronautics and Astronautics.

[27] Xiao, X., Edwards, J., and Hassan, H., 2004. "Blending Functions in Hybrid Large-Eddy/Reynolds-Averaged Navier-Stokes Simulations". *AIAA Journal,* ***42***(12), pp. 2508–2515.

[28] Hoaglin, D. C., Mosteller, F., and Tukey, J. W., 1983. *Understanding Robust and Exploratory Data Analysis*. John Wiley & Sons.

[29] Huber, P. J., and Ronchetti, E. M., 2009. *Robust Statistics*. John Wiley & Sons, Hoboken, New Jersey, USA.

[30] Celik, I., and Karatekin, O., 1997. "Numerical Experiments on Application of Richardson Extrapolation with Nonuniform Grids". *Journal of Fluids Engineering,* ***119***(3), pp. 584–590.

[31] Slater, J., 2021. Examining Spatial (Grid) Convergence. `https://www.grc.nasa.gov/www/wind/valid/tutorial/spatconv.html`. Accessed: Feburary 6, 2025.

[32] Eça, L., and Hoekstra, M., 2014. "A Procedure for the Estimation of the Numerical Uncertainty of CFD Calculations Based on Grid Refinement Studies". *Journal of Computational Physics,* ***262***, pp. 104–130.

[33] Rider, W., Witkowski, W., Kamm, J. R., and Wildey, T., 2016. "Robust Verification Analysis". *Journal of Computational Physics,* ***307***, pp. 146–163.

[34] Snedecor, G. W., and Cochran, W. G., 1989. *Statistical Methods*, 8th ed. Blackwell, Ames, Iowa.

[35] Oz, F., Kincaid, K., Delchini, M.-O. G., Gottiparthi, K. C., Glasby, R., and Curtis, F., 2025. "Comparison of Artificial Compressibility Methods for Coupled Laminar Fluid Flow and Heat Transfer". In AIAA SCITECH 2025 Forum, American Institute of Aeronautics and Astronautics.

[36] Glasby, R. S., 2024. "Point Creation for Anisotropic Adaptive Mesh Generation".